Forecasting the Coastal Ocean: Resolution, Tide, and Operational Data in the South Atlantic Bight

D. LYNCH AND K. SMITH

Dartmouth College, Hanover, New Hampshire

B. BLANTON, R. LUETTICH, AND F. WERNER

University of North Carolina, Chapel Hill, North Carolina

(Manuscript received 8 August 2003, in final form 1 December 2003)

ABSTRACT

This paper addresses shelf-scale simulation with dominant open-water boundary conditions obtained by inversion of interior data. Important, established operational data streams are located along the shore of the study area, in areas influenced strongly by the local geometry. Failure to properly resolve the modeled near field surrounding these data results in their incorrect interpretation, causing invalid inversions and erroneous field estimates far across the shelf. Specifically, improving the model fit to the unresolved data leads to skill degeneration farther offshore and generally unacceptable field estimates remarkably far from shore. Proper near-field resolution leads to valid interpretation and inversion of the same data, with high inverse skill apparent across the shelf. The resolution required is within reach of today's technology.

1. Introduction

Our objective is to construct a data assimilative forecast system in the South Atlantic Bight (SAB) shelf region, between St. Augustine, Florida, and Charleston, South Carolina, and offshore to roughly the shelf break (70–200-m isobath; Fig. 1a). Boicourt et al. (1998) provide a contemporary oceanographic review of these waters. Three-dimensional baroclinic physics are to be used on a high-resolution, local area mesh. Local forcings (river, wind, atmospheric heating, and stress) are to be applied directly, while remote or far-field baroclinic and barotropic motions are to be represented as boundary and/or initial conditions. Interior data are to be assimilated into the (local) forecast, causing appropriate adjustments to the least well known forcings. The target system is illustrated in Fig. 2. The most reliable interior data, from an operational point of view, are the established water level time series measured at the National Ocean Service (NOS) stations along the coast. In this study we take these data as given, and design toward their operational assimilation.

A primitive problem is the proper representation of the barotropic mode. Much of the observed motion on the shelf occurs in this mode, in the tide and weather bands. The former is completely a remotely driven process and must be represented by barotropic boundary conditions on the shelf. The wind-band dynamic is partly of local origin (direct response to surface pressure and traction) and partly of remote origin (propagation of the deep-sea pressure response to weather). Both responses propagate as hyperbolic disturbances across and along the shelf and interact with the topographic and hydrographic features there. So the barotropic boundary conditions need to be properly represented for the local domain; otherwise, these important motions cannot be properly simulated. A good prior or starting point, capturing something of the deep-sea reponse, is necessary, accompanied by a good inverse strategy for interpreting/inverting the local data. The local forward and inverse models need proper resolution and physical representation of the dominant processes; otherwise, the local data will be misinterpreted by the inversion and the model–data misfits assigned to incorrect causes. And while the barotropic mode is especially simple, errors in it will ruin all subsequent representations of more complex processes.

In this paper we examine the barotropic tidal dynamic in the subject region. There is a good prior, based on a far-field model with broad agreement with oceanic tides over the whole East Coast (CCAT Research Program 2003) and quality data along the coast (NOS 2002). In the inversion sense, the prior provides the tidal boundary conditions (BCs) to the forecast domain; the resulting misfit with data is reduced by adjusting the BCs. The

Corresponding author address: Dr. D. Lynch, Dartmouth College, 8000 Cummings Hall, Hanover, NH 03755-8000.
E-mail: daniel.r.lynch@dartmouth.edu

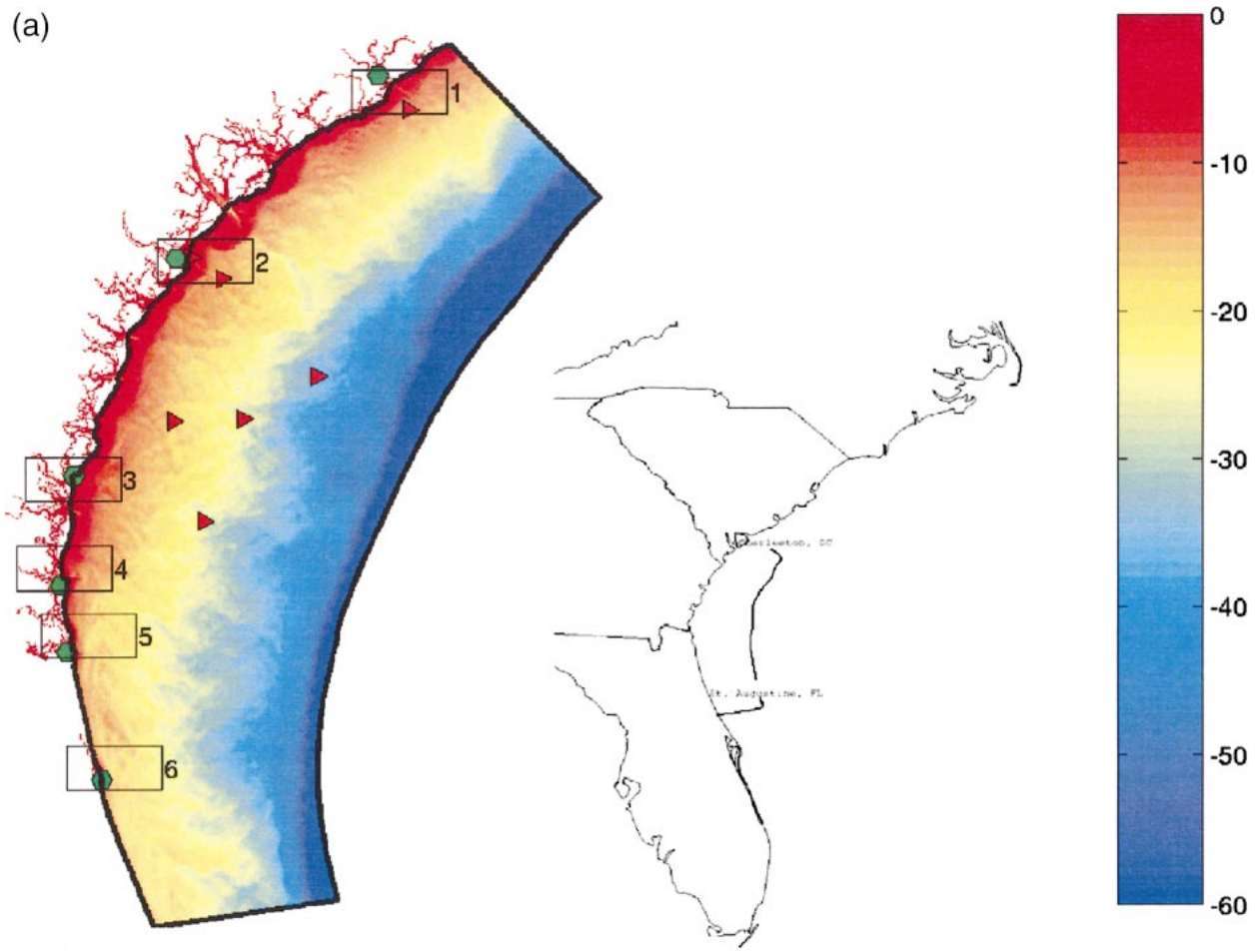

FIG. 1a. Study area and topography of the Peach domain. The bathymetric depth (m) is contoured. The position of the study area relative to state boundaries and the coastline is shown.

objective questions are (a) what resolution is needed, (b) how is inversion of the tidal signal constructed, (c) what level of fit is appropriate, and (d) what range of adjustment to the prior BC is justified?[1]

The importance of the tide should not be underestimated here. Currents and pressures on the shelf are dominated by it. The M2 elevation amplitude is of order 1 m; the phase range is 30° or 1 h. On the inner shelf, the M2 constituent accounts for 80%–90% of the observed velocity variability cross-shelf, 20%–40% of that along-shelf (Tebeau and Lee 1979; Lee and Brooks 1979). Equally important is the location of our principal operational data—along the shore, in several cases sequestered among the complex of estuaries and barrier islands. As we show, this has profound implications for the design of an operational forecast system. In the forecasting context, we need tidal predictions for the conventional oceanographic purposes (mixing, stratification, and tidal rectification); for the real-time interpretation of data, which is largely tidal; for the prediction of velocity, which depends heavily on the tidal mixing regime; and for the prediction of the water level, which is itself largely tidal and in which the tide phase is very influential in nonlinear modulation of episodic phenomena, for example, storms.

It is interesting to note that the *true* far-field tidal influence in this context is in fact time dependent. Modulation on seasonal and other time scales of standard tidal constituents on the shelf has been observed and reported, but not fully understood. Foreman et al. (2000) reported this phenomenon off Vancouver Island, British Columbia, Canada; while no physical explanation is offered, they were able to rule out any artifacts of the data processing. Similar observations are reported for the Yellow Sea by Kang et al. (1995, 2002) where the M2 phase modulation was of order 10°–15°, and a physical explanation is proposed in terms of two-layer dynamics. Our own processing of SAB data (Fig. 3a) confirms this

[1] Since the NOS data are already established, we leave open the important question of the design of observational networks, and look forward to future studies of this.

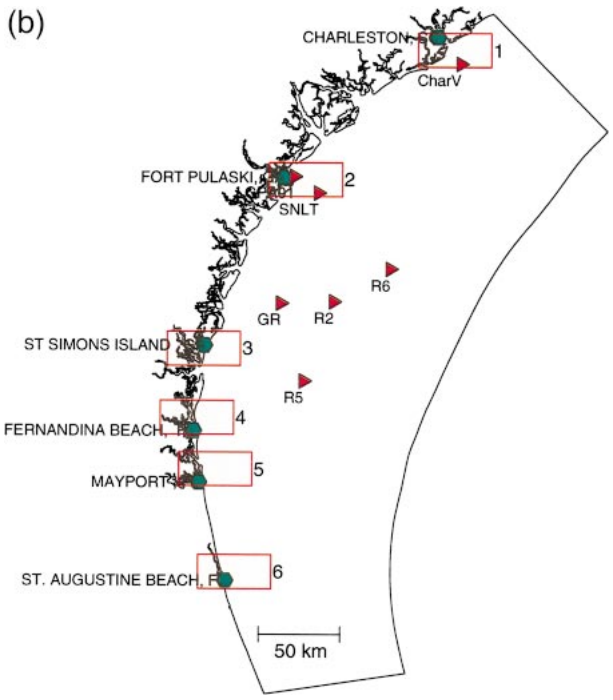

FIG. 1b. Data stations in the Peach domain. The named markers indicate the locations of six operational (dots) and seven nonoperational (triangles) stations. The numbered boxes are used throughout for detailed local display.

to be of order 5-cm amplitude and 5° phase[2] for the M2, with reasonable coherence across several stations. It remains formally an unexplained phenomenon. And while there appears to be a well-established mean annual cycle, the variance about it is comparable to the annual variance.

By contrast, the prior *model* of the far-field tides is typically a time-invariant spectrum of astronomical and shallow-water constituents, based on 2D physics and propagated shelfward from the deep ocean basin. Such a prior estimate cannot recognize these modulations or the interaction of far-field generation with in situ changes in hydrography, mixing, etc. Naturally, our prior is subject to continuous improvement, as the physical phenomena become better understood (Blanton et al. 2003, manuscript submitted to *J. Geophys. Res.*). But for operational purposes, this is presently the best prior estimate. It is indeed very good, and there will always be a better one later.

So, as in any forecasting context, we accept imperfection in the prior and correct for it by inversion of local (interior) data. Our bottom-line conclusions for this region are that an unusually high resolution of coastal features is needed for tidal fidelity; that inversions without this resolution create bogus solutions; and that tidal dynamics are heavily dependent on local, motion-dependent loss mechanisms. The effect of nearshore resolution is quantified in terms of its size and extent. The final tidal ''fit'' we achieve is demonstrably competitive, and the BC adjustments are within the range of uncertainty. We thus open the way to further investigations of wind-band and baroclinic forecast studies.

2. Previous modeling studies

Wang et al. (1984) examined the M2 tidal and wind-driven dynamics on the shelf from Cape Fear, North Carolina, to Cape Canaveral, Florida, and offshore to the 75-m isobath. The dynamics were 2D, constant density with 40-km resolution. Offshore boundary conditions were interpolated from Schwiderski (1980) at 1° resolution;[3] good agreement inshore was reached with Schwiderski in terms of elevation amplitude. Offshore velocity data also compared well with model predictions, but the accuracy degraded near the offshore boundary.

Werner et al. (1993) examined the tidal and subtidal dynamics on a similar domain, Cape Hatteras, South Carolina, to Cape Canaveral, and offshore to 70 m. The nearshore resolution reached as low as 2.8 km. Schwiderski's M2 results were specified at the open boundary; only qualitative tidal agreement is reported on the interior, due to uncertainties in the data and forcing. This model was linear, diagnostic, and three-dimensional.

Chen et al. (1999) modeled a similar domain, 28.5°–34.5°N, and offshore to the 200-m isobath, with the similar objective of representing the subtidal processes. The resolution was 2–3 km cross-shelf, 4–6 km alongshelf. This model was 3D and nonlinear, with 16 vertical surfaces, and Mellor–Yamada–Galperin level 2.5 turbulence (Mellor and Yamada 1982; Galperin et al. 1988). The tidal calculation was idealized with uniform density and the three main semidiurnal tides were considered: M2, N2, and S2. Offshore boundary conditions were from Egbert et al. (1994) (0.5° resolution). The amplitude and phase agreement are reported at three coastal locations, with a precision of 1–2 cm and 1° phase for the M2. (As above, the observed M2 amplitude is of order 1 m; the phase range is 30°.) This paper reports an agreement in amplitude, but not phase, with calculations forced by Schwiderski's (1980) boundary conditions, and favors the more precise Egbert et al. conditions.

All of the above studies were done in ''hindcast'' or ''simulation'' mode and focused mainly on subtidal phenomena. The role of the modeled tide is to generate nonlinear mixing fields and tidally rectified currents.

Zhang et al. (2002) present a forecast model for the shelf from Cape Breton, Nova Scotia, Canada, to Cape

[2] For a periodic signal, at 1-m amplitude, 1° of pure phase discrepancy is equivalent to 1.745 cm of pure amplitude discrepancy, in terms of rms time domain misfit.

[3] For comparison purposes, in this region, 0.1° (lat, lon) = (11.16, 9.72) km.

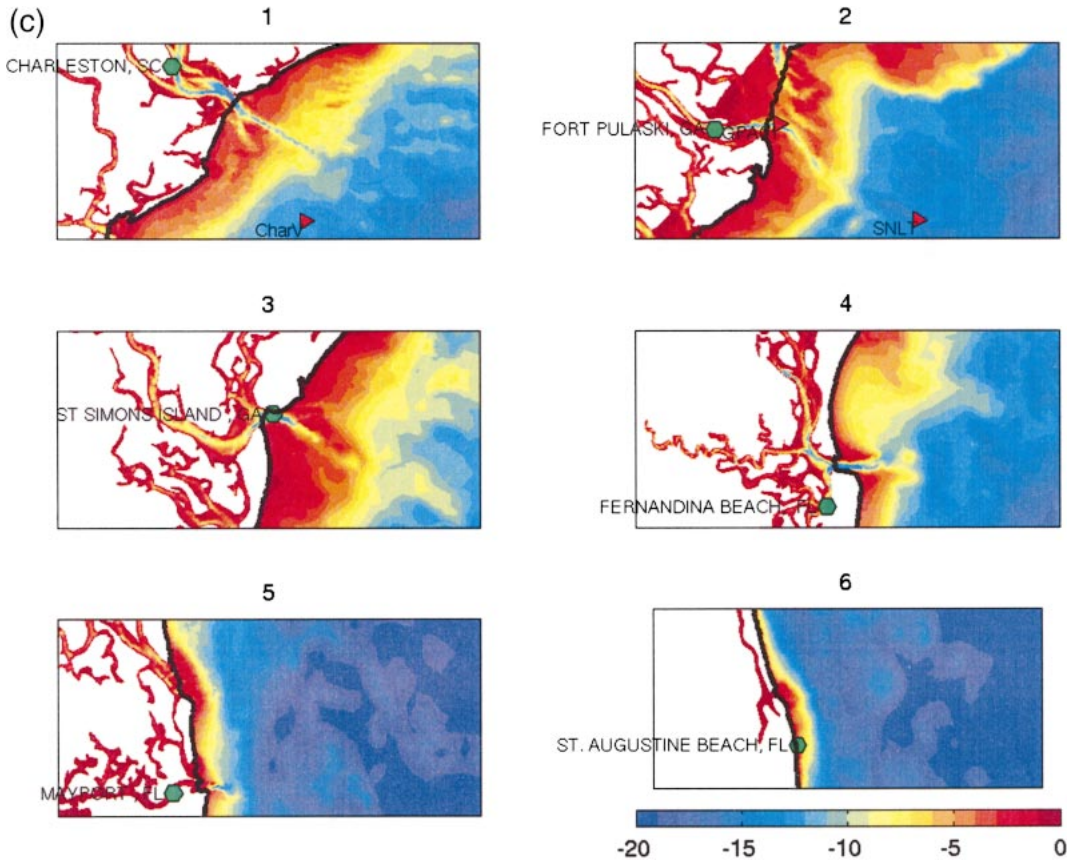

FIG. 1c. Local topographic details (m) near the operational stations. The dark black line is the shoreward termination of the ''no bays'' mesh. The horizontal axis of each frame is 45 km. The length scale is the same as in Figs. 3b, 5b, 6b, 7b, 8b, 9b, and 10b.

Canaveral, with offshore BCs specified on a wide arc conneting the two across the North Atlantic. Typical resolution is 5 km nearshore, 30 km offshore. This is a linear, 2D model and the study focuses exclusively on wind-band dynamics. Accordingly, the data and model forcings are detided before use (details of this are not given; one presumes known tide-band priors for all data). An adjoint method is used to improve the fit at 18 coastal NOS water-level stations, the prior is driven by an analyzed meteorological field, and the control variables are the wind drag coefficients (16 degrees of freedom). Offshore boundary conditions are not clear in this study.

3. Our domain

Figure 1 shows the forecast domain. It includes a slice of the continental shelf roughly 420 km long, terminating offshore at the 200-m isobath, (roughly 100 km offshore). The topography is from the National Oceanic and Atmospheric Administration (NOAA) Coastal Relief Model (NNDC 2002a,b). Figure 3 shows the baseline mesh (Peach2.). There are 100 823 triangles and 57 824 horizontal nodes. The graded mesh includes reasonable resolution (500 m) of the inshore/estuarine topography, with *250-m resolution* near the operational NOS data stations. Outside of the estuaries, the graded resolution is depth dependent with uniform Courant number (triangle area proportional to depth). At the seaward boundary, the resolution is roughly 5 km. There are 21 vertical levels everywhere, with vertical resolutions of 1 m in the surface and bottom boundary layers. The mesh is projected onto an f plane for computational purposes. There are about 200 open boundary nodes.

4. Our data

Table 1 records the M2 data and locations that we use. There are six operational sea level stations where publicly available time series are available in real time (NOS 2002). These are the data that we expect to employ operationally. Each has a published value of M2 amplitude and phase, based on a local, historical time series analysis, which is listed in Table 1. We refer to these as the operational or ''active'' data stations; they are candidates for real-time assimilation and we will use them that way here.

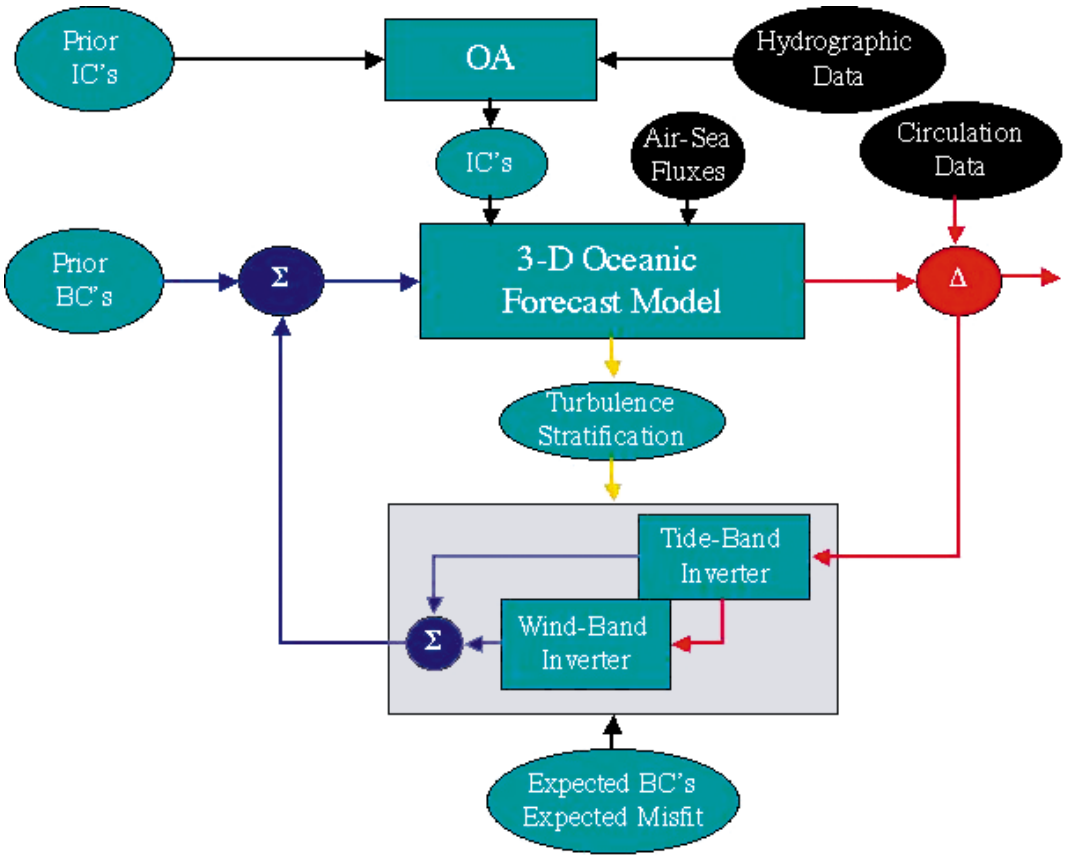

FIG. 2. The target system for the SAB forecasting system. The two inverters assign hydrodynamic misfits to the boundary conditions in the tide and wind bands serially. These models are described in Lynch and Naimie (2002). Here, OA indicates an objective analysis step (Lynch and McGillicuddy 2001). This paper deals with the tide-band inversion loop exclusively.

Also shown in Table 1 are seven additional stations where we have reliable M2 constituents. These are either unavailable or less reliable in a forecast mode but useful here as verification data for these nonoperational experiments. These stations are universally farther offshore than the operational stations, with stations R2, R5, and R6 well into the midshelf region. As such we expect them to be less sensitive to shoreward resolution. They are designated as ''passive'' stations. Herein, passive data are used for verification but are not actively assimilated.

Figure 1c shows these data locations on the gridded Peach2 topography. The operational data are generally inshore, behind and among important topographic features including barrier islands, channels, and other estuarine features. Implications of this are central to this study and are discussed below.

Figure 1c also shows the truncation line for a second mesh, Peach2NB, which is congruent with Peach2 but with the estuarine elements deleted. Peach2NB terminates near shore in the same spirit as meshes used in previous studies, although here the resolution is higher, 500 m.

5. Our model

We use the tidal model of Lynch and Naimie (1993, hereafter LN93). This is a nonlinear 3D model of the standard hydrostatic, constant-density shallow-water equations, on an f plane. The discretization is harmonic in time, and finite element in space with linear triangles providing variable resolution. Nonlinearities are accommodated iteratively. In the present calculations, M2 forcing alone is enforced at the oceanic boundaries; there is no mass flux across the landward boundaries.

Vertical turbulence is represented in eddy-viscosity form, with the same closure as is used in LN93: a quadratic bottom stress law based on the near-bottom velocity,

$$N\frac{\partial \mathbf{v}}{\partial z} = C_d|\mathbf{v}|\mathbf{v},$$

and a motion-dependent representation of vertical eddy viscosity based on the local vertically averaged current speed,

$$N(x, y, t) = N_0|\overline{\mathbf{v}}|^2$$

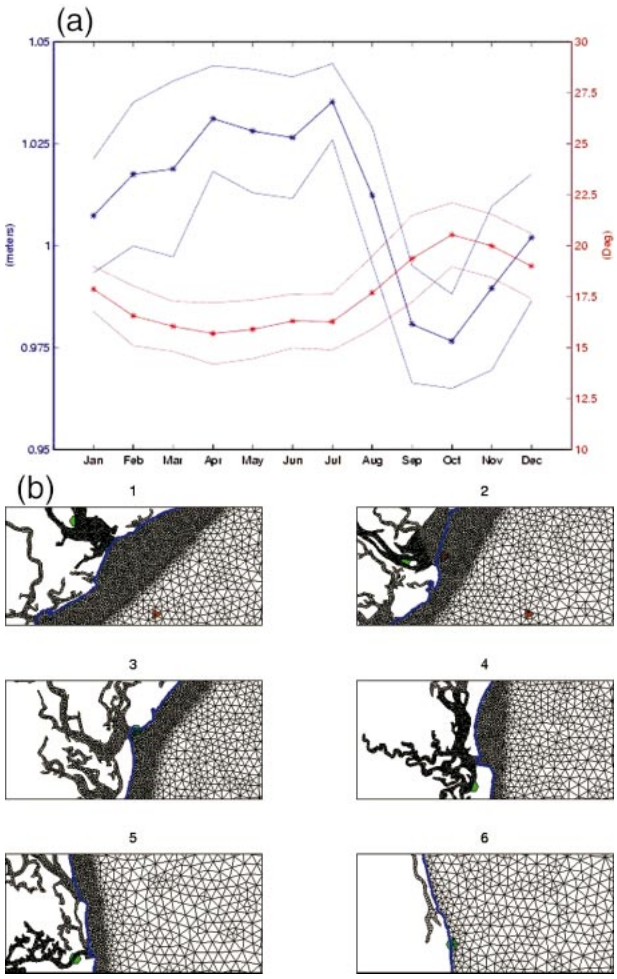

FIG. 3. (a) The M2 amplitude and phase at Fort Pulaski, GA, estimated by monthly harmonic analyses for 10 yr. The means for each month were binned to produce the climatological mean (lines with asterisks) and standard deviation (lines without asterisks). Short record months were skipped. (b) Peach2 mesh details near the operational stations. The solid blue line is the shoreward termination of the Peach2NB mesh.

(N is the vertical viscosity, C_d the bottom drag coefficient, $\mathbf{v}$ the velocity sampled at the bottom, and $|\overline{\mathbf{v}}|$ the vertically averaged velocity). The baseline values of the two parameters (C_d, N_0) are the same as in LN93: (0.005, 0.2, respectively) in the MKS system. These two parameters are constant spatially and temporally. The 21 vertical surfaces are arranged to provide 1-m resolution in the surface and bottom boundary layers, regardless of total depth, as in previous studies with this closure. There is no horizontal eddy viscosity.

In harmonic terms, this M2 calculation is particularly simple; the principal nonlinearity involves the nonlinear turbulence closure. The speed dependence here turns out to be critical, providing spatial structure generated by the motion itself, with no further spatially variable parameterization. In time domain models the contemporary standards commonly invoke more sophisticated closures; our own and others' (e.g., Davies and Xing 1995) experiments show the effectiveness of this closure vis-à-vis barotropic tidal dynamics, and this is certainly adequate in the present system design context. However, we do not advocate this simpler closure for ultimate forecasting purposes where atmospheric heating and freshwater forcing are important.

The model–data misfit is quantified as the difference in complex tidal amplitude, Z:

$$Z = Ae^{-i(\pi/180)\varphi},$$

with (A, φ) the conventional, real-valued amplitude and the phase lag in degrees; Z has the same units as A. Misfits are the complex difference between modeled (Z_m) and observed (Z_o) complex amplitudes. The fit is quantified in terms of the mean squared misfit,

$$\frac{1}{N}\sum |Z_m - Z_o|^2,$$

or its rms equivalent.

6. The prior forcing

Prior conditions along the open boundary are taken directly from a multiconstituent, regional tidal database

TABLE 1. The M2 data and locations; amplitude (m) and phase (°). The top group lists the operational stations; they will be active in the inversion. The bottom group lists the passive stations; they will be used to verify the inversion.

Station name	Lat (°)	Lon (°)	Amplitude	Phase
St. Augustine Beach, FL	29.856667	−81.263333	0.662	14.30
Mayport, FL	30.393333	−81.431667	0.662	28.10
Fernandina Beach, FL	30.671667	−81.465000	0.898	32.90
St. Simons Island, GA	31.131667	−81.396667	0.975	23.80
Fort Pulaski, GA	32.033333	−80.901667	1.013	17.90
Charleston, SC	32.781667	−79.925000	0.783	10.40
CharV	32.640000	−79.780000	0.710	357.00
GPA01	32.038300	−80.831700	0.950	9.50
SNLT	31.950000	−80.680000	0.890	6.30
R6	31.543000	−80.224000	0.700	3.40
R2	31.367000	−80.582000	0.780	5.90
GR	31.358600	−80.916700	0.880	9.50
R5	30.939900	−80.771000	0.760	8.00

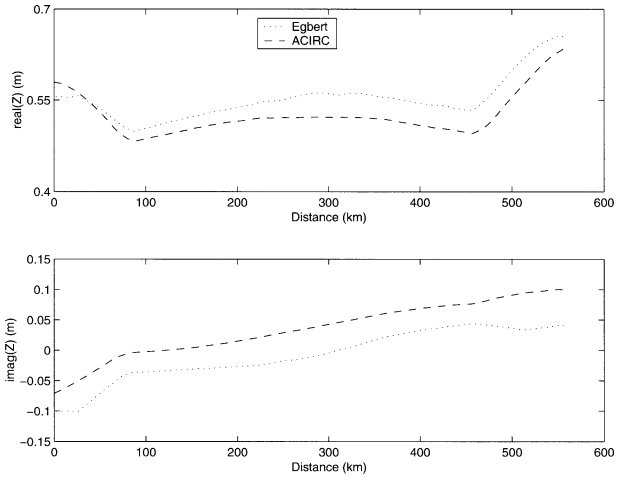

FIG. 4. Prior M2 boundary conditions from two sources: CCAT Research Program (2003) (used in the present study) and Egbert et al. (1994). The real and imaginary parts of the complex M2 amplitude are shown (m), as a function of boundary position. The boundary corners are easily identified. For completeness, the older, coarser prior of Schwiderski (1980) gives three complex amplitudes in the region: (0.649, −0.262), (0.850, −0.228), and (0.796, −0.084).

generated using the 2D, barotropic Advanced Circulation (ADCIRC) finite-element model (CCAT Research Program 2003). These appear in Fig. 4. They represent the windless version of an operational product, which we will use later as input to operational shelf forecasts. This product has been extensively used for related purposes all along the U. S. East Coast (Mukai et al. 2002). Also shown for comparison are the equivalent priors drawn from the databases used in previous studies. Among the conclusions to be drawn from these are that (a) the spatial scale of variation is of order 0.20 m over 500 km; (b) about half of this variation occurs across-shelf, at a length scale of 70 km; (c) the variation among competing priors is of order 0.05 m; and (d) this variation is comparable to the expected seasonal variation, making greater prior precision unlikely in the near term without settling and modeling the responsible physical mechanisms. Overall, an adjustment of this prior so that a good local model reproduces observed local dynamics is justified within the above-mentioned size range.

Now, this unknown tidal forcing is small relative to the overall tidal signal (1 m). But it is big relative to the wind-band signal, which is of order 0.10 m. This unfavorable signal-to-tide ratio makes it easy to bogus the wind-band variability unless the tides are very precise—hence the need for inverse deduction even in the tide band.

7. Results

a. Prior

First we examine the ''prior'' simulation results, that is, without inversion. The solution is shown in Fig. 5.

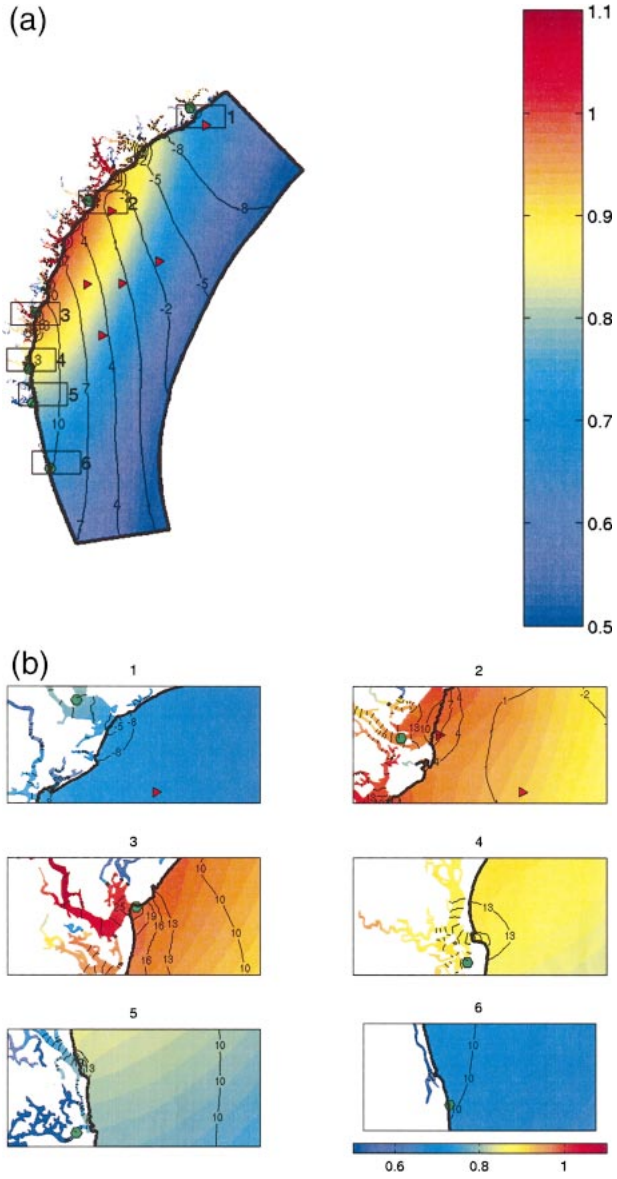

FIG. 5. (a) The M2 tidal solution on Peach2 mesh, prior to inversion. The color shading interval for the amplitude (m) represents 1 cm and the contour interval for the phase isolines is 3°. (b) Prior M2 solution on the Peach2 mesh: detail at the operational stations. Figures 5, 6, 8 and 9 follow the same convention.

There is broad qualitative agreement with the data. There is a general shoreward amplification and a general increase in phase lag toward the southwest. In particular we observe a near-field effect at the coastal estuaries, with a length scale of order 25 km and a size of 0.10 m. The quantitative fit with the data is shown in Tables 2 and 3. This fit is quite good, with the mean misfit size being about 0.06 m. Contributing to this is a phase bias all across the domain: the computed solution has universally lower phase lag, averaging about 4°. Especially telling are the offshore phase errors. The three stations that are close to the open boundary show this bias clear-

TABLE 2. Prior and posterior solutions, by station. Amplitude (amp), m; phase, (°). Misfit (|z−z_obs|, m) is as defined in the text: the absolute value of the complex difference in the complex amplitude. Model outcomes and misfits are evaluated at the node nearest the data location.

	Peach2			Peach2NB		
Station	|z−z_obs|	Amp	Phase	|z−z_obs|	Amp	Phase
Prior						
St. Augustine Beach, FL	0.0495	0.673	10.16	0.0639	0.682	9.12
Mayport, FL	0.0686	0.662	22.16	0.2729	0.798	9.36
Fernandina Beach, FL	0.0243	0.886	31.55	0.3693	0.851	8.71
St. Simons Island, GA	0.0194	0.987	22.90	0.2846	0.950	6.86
Fort Pulaski, GA	0.0604	0.969	15.51	0.3779	0.903	356.11
Charleston, SC	0.0904	0.778	3.77	0.2824	0.681	349.63
CharV	0.0819	0.698	350.41	0.0932	0.677	349.80
GPA01	0.0407	0.965	7.24	0.2217	0.902	356.07
SNLT	0.0970	0.921	0.47	0.1597	0.871	355.97
R6	0.0720	0.701	357.51	0.0922	0.686	355.86
R2	0.0588	0.788	1.64	0.0941	0.770	358.98
GR	0.0639	0.896	5.50	0.1223	0.871	1.51
R5	0.0449	0.773	4.79	0.0760	0.764	2.28
Posterior						
St. Augustine Beach, FL	0.0145	0.665	13.07	0.0825	0.618	20.57
Mayport, FL	0.0396	0.661	24.67	0.0939	0.754	26.75
Fernandina Beach, FL	0.0196	0.888	33.99	0.1120	0.823	27.35
St. Simons Island, GA	0.0321	0.992	25.39	0.0587	0.961	27.18
Fort Pulaski, GA	0.0358	0.977	17.98	0.0411	0.991	15.92
Charleston, SC	0.0221	0.785	8.79	0.0590	0.780	6.08
CharV	0.0256	0.708	354.93	0.1359	0.771	6.42
GPA01	0.0264	0.976	9.73	0.1148	0.990	15.86
SNLT	0.0689	0.932	2.89	0.1615	0.952	15.58
R6	0.0500	0.714	359.50	0.1498	0.745	14.75
R2	0.0357	0.799	3.69	0.1756	0.815	18.28
GR	0.0385	0.906	7.70	0.1874	0.911	21.34
R5	0.0246	0.780	6.89	0.1729	0.774	20.90

ly. They also reveal a north–south trend in phase misfit: R6 (5.9°), R2 (4.3°), R5 (3.2°).

The most likely reason for this structured bias is a relatively uniform phase error introduced in the prior boundary conditions. Since these originate from a much larger scale calculation, unbiased errors at these length scales will appear to be relatively constant locally. So we are justified in inverting this misfit for a local BC correction. Also, this Peach2 prior misfit is in the envelope of the observed but unexplained tidal modulation, which adds additional strength to this justification.

We noticed in similar simulations (not shown) that reducing the closure to a linear form produced unsatisfactory results, unless we introduced unacceptable spatial variations in the loss parameters. Given the good speed-dependent results shown here, achieved with a constant spatial parameterization with literature values, we conclude that the speed dependence is quite essential. Invention of additional, spatially dependent parameters is not justified.

The same simulation without the local mesh details, on the Peach2NB mesh, appears in Fig. 6 and is much less satisfying. It lacks completely the small-scale near-field effects. The misfit is reported in Tables 2 and 3.[4] It is perhaps reasonable offshore, 0.12 m, but is still deficient relative to the Peach2 case above. But it grows to significant levels as we approach the operational NOS stations where the mean misfit is 0.275 m—one-fourth of the signal. This misfit is neither acceptable nor explainable without posing serious questions about the data quality (and we reject a data challenge here).

Figure 7 presents the difference between these two prior solutions. The mismatch between the two solutions is significant, of order 0.05–0.10 m all across a broad

TABLE 3. Mean absolute value of surface elevation misfits (from Table 2) and boundary adjustments for four different simulations. (Units: m.) Note that by definition, the misfit measures complex amplitude; it blends both amplitude and phase information.

	Active misfit	Passive misfit	Boundary adjustment
Simulation	|z−z_obs|	|z−z_obs|	|z−z_prior|
Peach2 Prior	0.052	0.066	0
Peach2NB Prior	0.275	0.123	0
Peach2 Posterior	0.027	0.039	0.033
Peach2NB Posterior	0.075	0.157	0.132

[4] Misfits are evaluated on a ''nearest node'' basis. For the Peach2NB solutions this is a potential concern; but Fig. 6b shows that these solutions are in fact very smooth near the shore gauges. Hence, the misfit metrics are insensitive to the detailed location of the comparison point.

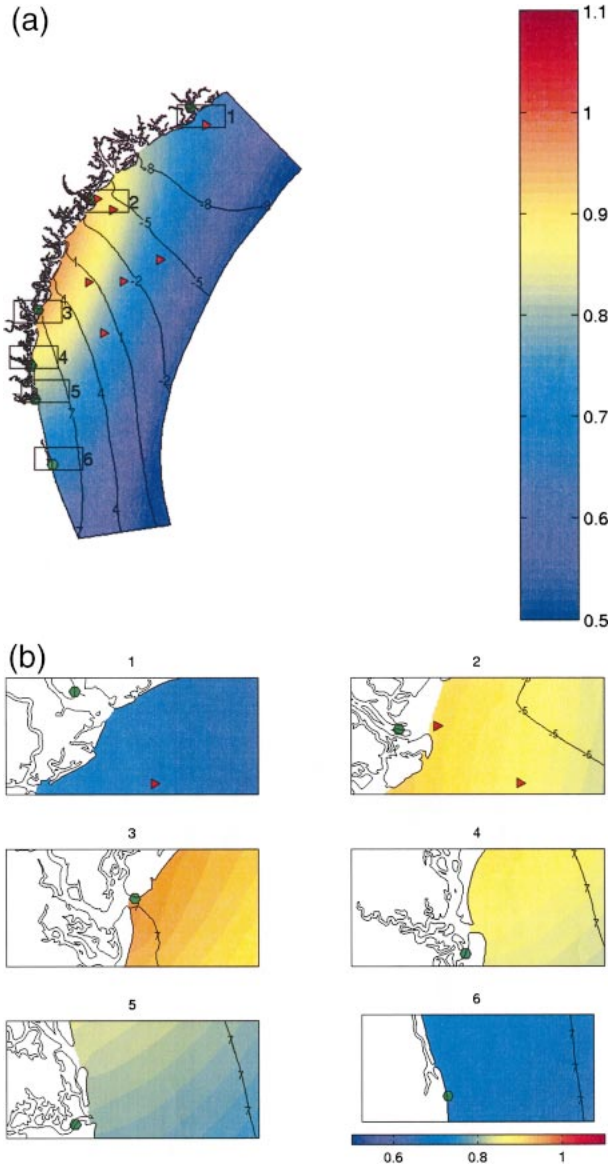

FIG. 6. (a) Prior M2 solution on the Peach2NB mesh. (b) Local detail.

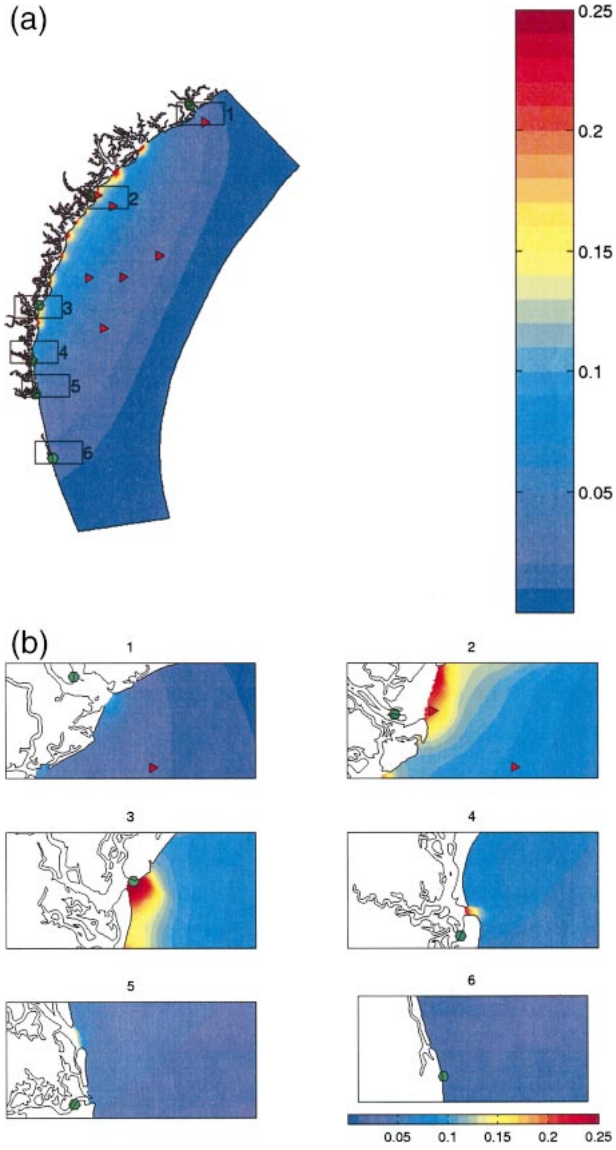

FIG. 7. (a) Difference between the two priors: absolute value of the complex M2 amplitude difference (m). The color shading represents interval 1 cm. Figure 10 follows the same convention. (b) Local details of the difference shown in (a) between the two priors.

coastal area, and peaking shoreward at the operational sites at roughly 0.25 m. In the north, the discrepancy is mainly in amplitude (not shown). This gives way to a dominant phase discrepancy in the center of the domain. In the south, where the topography is largely uncomplicated, both meshes perform about the same. At the boundaries, of course, there is no discrepancy.

The only factor separating these simulations is the shoreward resolution. The prime operational data are immersed in this difference.

b. Posterior

Next we invert the NOS data to produce adjustments in the prior boundary conditions. The procedure is that of Lynch et al. (1998), using the 3D model Truxton. This is a linearized version of the forward model; the principal nonlinearity, the motion-dependent friction, was retained. The weighted least squares option was used to reduce the elevation misfit at the NOS stations. All other data were passive, that is, used for verification only. Regularization was used to penalize the size and slope of the boundary adjustments. There are three parameters: expected size of elevation misfit, 0.005; expected size of boundary adjustment, 0.01; and expected slope of boundary adjustment, 10^{-7} (All units are MKS.) These three metrics were all weighted equally in the minimization. They are consistent with prior estimates of these quantities, within the same factor of about 5.

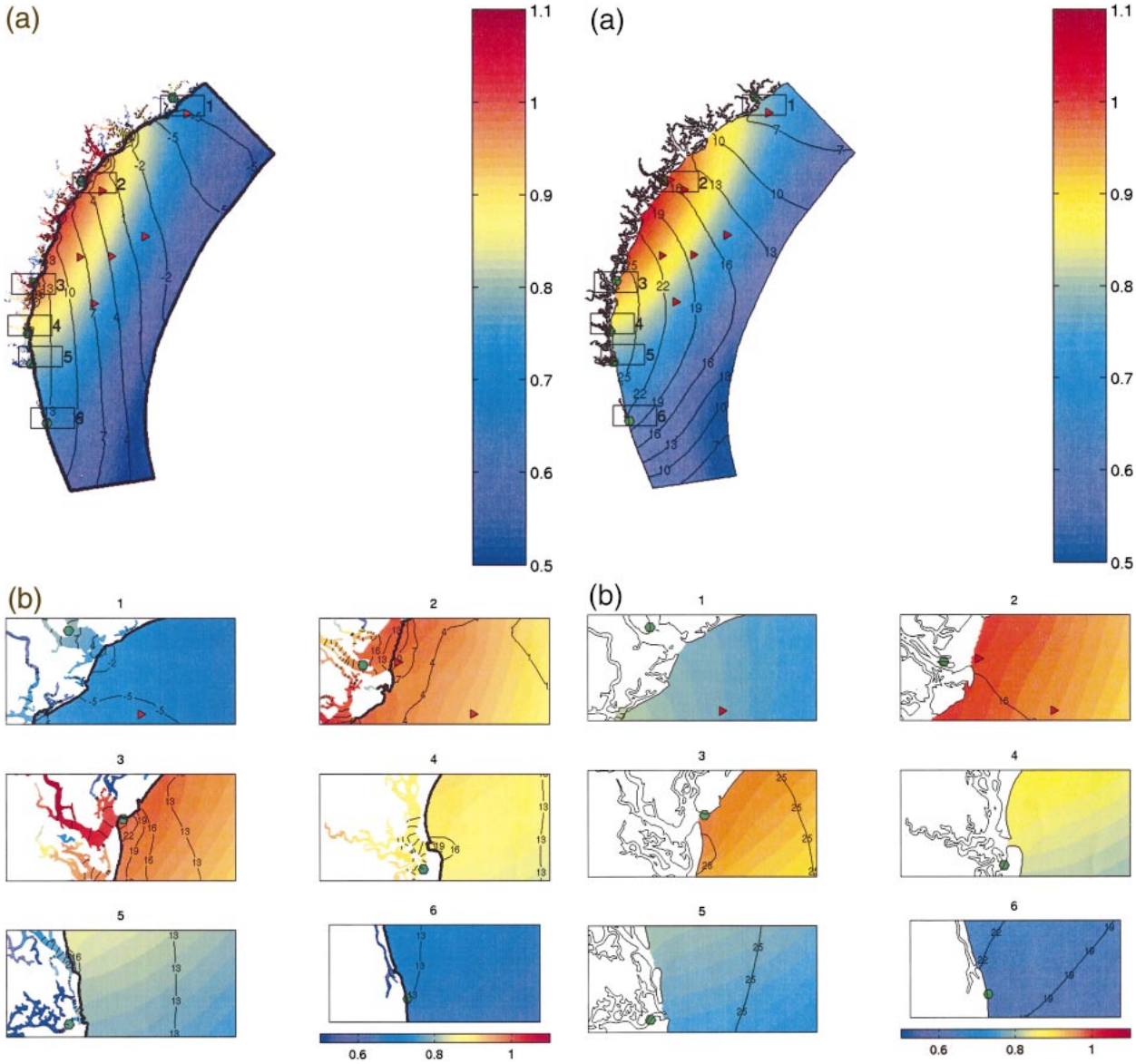

FIG. 8. (a) Postinversion M2 solution on the Peach2 mesh. (b) Local details.

FIG. 9. (a) Postinversion M2 solution on the Peach2NB mesh. (b) Local details.

A fourth parameter, the singular value decomposition (SVD) condition number cutoff for the normal equations, was set very low at 10^{-12} to achieve high-rank inversions.

The results for Peach2 and Peach2NB appear in Figs. 8–10, and the misfits are reported in Tables 2 and 3. The Peach2 posterior is a competitive and credible fit to both the active and passive data: mean misfits of 0.027 (active) and 0.039 m (passive), almost halving the prior misfits. This is achieved with a mean adjustment at the boundary of 0.033 m. The apparent phase bias is removed, and we obtain a nearly seamless solution quality both inshore and offshore. In fact the principal adjustment to the prior forcing is this phase shift. Overall this is a successful inversion.

The Peach2NB results remain unacceptable after inversion. There is a significant improvement in fit at the active NOS stations (0.075 m, down from 0.275 m). But the fit offshore at the passive stations was degraded (0.157 m, up from 0.123 m), and large, unjustified adjustments (0.132 m) had to be made to the boundary conditions. This is undeniable evidence of a failed inversion; we are fitting data for the wrong reasons, and creating big problems elsewhere.

Figure 10, the difference between the two posterior solutions, compares our best estimate of truth—the valid Peach2 inverse solution—with the mistaken estimate

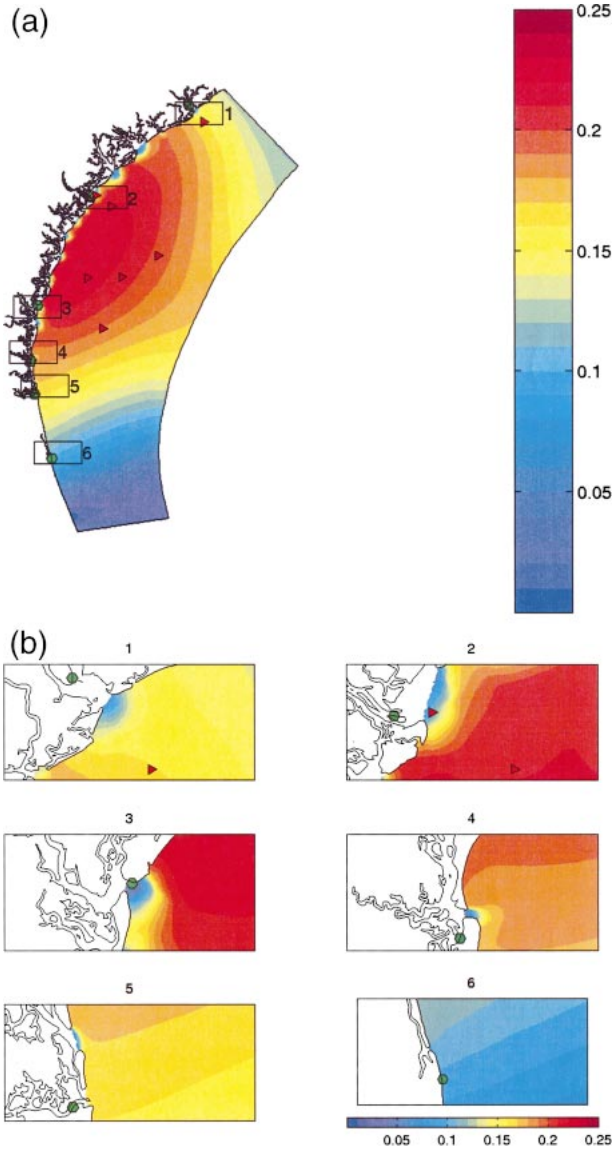

FIG. 10. (a) Difference between the two postinversion solutions. Absolute value of the complex amplitude difference (m). (b) Local details from (a).

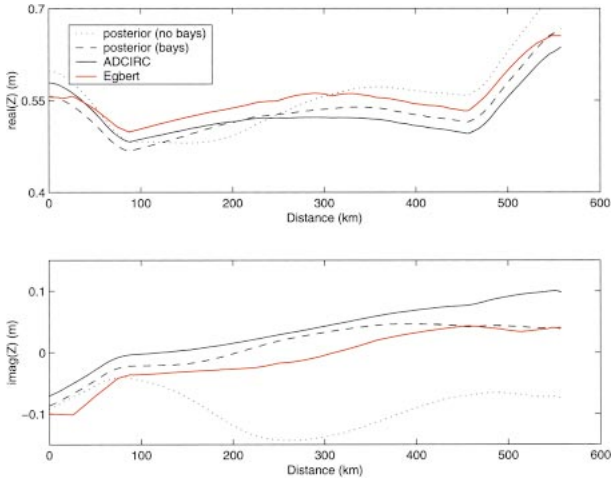

FIG. 11. Two different prior estimates of boundary conditions, and the two posterior estimates generated herein. The real and imaginary parts of the M2 amplitude are plotted separately.

from the otherwise comparable Peach2NB inversion. Their difference is an estimate of how far wrong we could go if the latter were accepted. Figure 10 retains some features from the comparable Fig. 7 (the difference between priors). Notably, there is a large zone of discrepancy in the interior and shoreward. Here it reaches 0.20 m over a significant part of the nearshore area, while maintaining the minimized misfit of 0.075 m (mean) at the NOS stations. One can see a strong spatial distortion near these stations. Offshore at the passive data stations we clearly see that the 0.157-m misfit there represents the error of a misguided inversion. And while the priors were constrained to agree along the open boundary, the posteriors do not and an error of order 0.10 m is propagated to the boundary by this inversion. Clearly, we bear a heavy penalty for failing to resolve the estuaries. The forecast field is ruined all the way out across the shelf.

The posterior boundary adjustments are plotted in Fig. 11. The Peach2 result is within the uncertainty of the prior; the Peach2NB result is anomalous, consistent with the above discussion.

The conclusion here is simple: *resolve the physics in the region of the data.* Otherwise, unresolved misfits will be incorrectly assigned by inversion to inappropriate solution features all over the shelf. And this would be masked by an unjustified misfit reduction—the appearance of quality. Given the locations of our operational data, we have a clear requirement for high local forecast resolution.

8. Conclusions

In the present forecasting context, we need to invert interior observations to find tidal adjustments to necessarily imperfect prior boundary conditions. The tidal adjustment is small but important; the critical subtidal phenomena are the same general size as these tidal adjustments. And the tidal adjustment must be done routinely, as it is not understood or predictable.

The only reliable operational data are ''hiding'' in the inshore topographic details. Failure to provide adequate resolution leads in one of two directions:

- ignore the serious misfits at unresolved locations and accept a significant distortion in the computed near field, which has surprisingly large spatial extent; or
- worse yet, reduce the unresolved misfits via inversion and create erroneous solution features all over the shelf. This fact would be masked by an unjustified misfit reduction.

In either case the forecast is ruined. Our Peach2NB results represent a serious prior misfit and a wild and unphysical inversion that spoils the fit to passive data (those not targeted by the inversion). This is simply not credible, a classic case of getting the right answer (fitting the active data) for the wrong reasons, creating and disguising serious far-field errors in the process. On the contrary, adequate resolution—herein, our Peach2 solution—leads to good quality prior solutions. Coupling these with a properly designed inversion leads to posterior solutions that meet contemporary misfit standards, proper data interpretation, and valid forecast fields.[5]

So inshore resolution is absolutely necessary. Here we have achieved this with unstructured meshes of triangles; in our experience that is the natural way forward, although nothing here precludes the use of other numerical methods. The resolution needed—0.250 km near shore, nested in a basin-scale prior model of the North Atlantic—is readily achievable with contemporary machines, networks, and algorithms.

Acknowledgments. This work was supported by NASA, as part of the National Ocean Partnership Program.

REFERENCES

Boicourt, W. C., W. J. Wiseman, A. Valle-Levinson, and L. P. Atkinson, 1998: Continental shelf of the southeastern United States and the Gulf of Mexico: In the shadow of the western boundary current. *The Sea*, A. R. Robinson and K. H. Brink, Eds., Regional Studies and Syntheses, Vol. 11, Wiley and Sons, 135–182.

CCAT Research Program, cited 2003: ADCIRC tidal databases. Version ec_95 d. [Available online at http://www.marine.unc.edu/C_CATS/tides/tides.htm.]

Chen, C., L. Zheng, and J. O. Blanton, 1999: Physical processes controlling the formation, evolution, and perturbation of the low-salinity front in the inner shelf off the southeastern United States: A modeling study. *J. Geophys. Res.*, **104** (C1), 1259–1288.

Davies, A. M., and J. Xing, 1995: An intercomparison and validation of a range of turbulence closure schemes used in three dimensional tidal models. *Quantitative Skill Assessment for Coastal Ocean Models*, D. R. Lynch and A. M. Davies, Eds., Coastal and Esturine Series, Vol. 47, Amer. Geophys. Union, 71–95.

Egbert, G. D., A. F. Bennett, and M. G. G. Foreman, 1994: TOPEX/POSEIDON tides estimated using a global inverse model. *J. Geophys. Res.*, **99,** 24 821–24 852.

Foreman, M. G. G., R. E. Thompson, and C. L. Smith, 2000: Seasonal current simulations for the western continental margin of Vancouver Island. *J. Geophys. Res.*, **105** (C8), 19 665–19 698.

Galperin, B., L. H. Kantha, S. Hassid, and A. Rosati, 1988: A quasi-equilibrium turbulent energy model for geophysical flows. *J. Atmos. Sci.*, **45,** 55–62.

Kang, S. K., J.-Y. Chung, S.-R. Lee, and K.-D. Yum, 1995: Seasonal variability of the M2 tide in the seas adjacent to Korea. *Cont. Shelf Res.*, **15,** 1087–1113.

——, M. G. G. Foreman, H.-J. Lie, J.-H. Lee, J. Cherniawsky, and K.-D. Yum, 2002: Two-layer tidal modeling of the Yellow and East China Seas with application to seasonal variability of the M2 tide. *J. Geophys. Res.*, **107,** 3020, doi:10.1029/2001JC000838.

Lee, T. N., and D. Brooks, 1979: Initial observations of current, temperature, and coastal sea level response to atmospheric and Gulf Stream forcing. *Geophys. Res. Lett.*, **6,** 321–324.

Lynch, D. R., and C. E. Naimie, 1993: The M2 tide and its residual on the outer banks of the Gulf of Maine. *J. Phys. Oceanogr.*, **23,** 2222–2253.

——, and D. J. McGillicuddy Jr., 2001: Objective analysis for coastal regimes. *Cont. Shelf Res.*, **21,** 1299–1315.

——, and C. E. Naimie, 2002: Hindcasting the Georges Bank circulation. Part II: Wind-band inversion. *Cont. Shelf Res.*, **22,** 2191–2224.

——, ——, and C. G. Hannah, 1998: Hindcasting the Georges Bank circulation. Part I: Detiding. *Cont. Shelf Res.*, **18,** 607–639.

Mellor, G. L., and T. Yamada, 1982: Development of a turbulence closure model for geophysical fluid problems. *Rev. Geophys. Space Phys.*, **20,** 851–875.

Mukai, A. Y., J. J. Westerink, R. A. Luettich Jr., and D. Mark, 2002: Eastcoast 2001: A tidal constituent database for the western North Atlantic, Gulf of Mexico and Caribbean Sea. Tech. Rep. ERDC/CHL TR-02-24, U.S. Army Engineer Research and Development Center, Coastal and Hydraulics Laboratory, Vicksburg, MS, 201 pp.

NNDC, 2002a: Coastal relief model: East Coast, Vol. 2. NOAA National Data Centers, CD-ROM.

——, 2002b: Coastal relief model: Florida and eastern Gulf of Mexico. Vol. 5. NOAA National Data Centers, CD-ROM.

NOS, cited 2002: Harmonic tidal data. [Available online at http://coops.nos.noaa.gov/data_retrieve.shtml?input_code=100201001har.]

Schwiderski, E. W., 1980: On charting the global ocean tides. *Rev. Geophys. Space Phys.*, **18,** 243–268.

Tebeau, P. A., and T. N. Lee, 1979: Wind induced circulation on the Georgia shelf. Tech. Rep. 79003, University of Miami, Miami, FL, 177 pp.

Wang, J. D., V. Kourafalou, and T. N. Lee, 1984: Circulation on the continental shelf of the southeastern United States. Part II: Model development and application to tidal flow. *J. Phys. Oceanogr.*, **14,** 1013–1021.

Werner, F. E., J. O. Blanton, D. R. Lynch, and D. K. Savidge, 1993: A numerical study of the continental shelf circulation of the U.S. South Atlantic Bight during the autumn of 1987. *Cont. Shelf Res.*, **13,** 971–997.

Zhang, A., B. B. Parker, and E. Wei, 2002: Assimilation of water level data into a coastal hydrodynamic model by an adjoint optimal technique. *Cont. Shelf Res.*, **22,** 1909–1934.

[5] We are aware of previous studies that appear to fit fewer data points even better, at lower resolution, and that show qualitatively different tidal maps. This appears to be consistent with the findings here.